Journal of Power Sources 196 (2011) 4012–4018

Contents lists available at ScienceDirect

Journal of Power Sources

journal homepage: www.elsevier.com/locate/jpowsour

New molten salt systems for high temperature molten salt batteries: Ternary and quaternary molten salt systems based on LiF–LiCl, LiF–LiBr, and LiCl–LiBr

Syozo Fujiwara [a,*], Minoru Inaba [b], Akimasa Tasaka [b]

[a] Technology Development Center, Energy Company, Panasonic Corporation, Matsushita-cho, Moriguchi, Osaka 570-8511, Japan
[b] Department of Molecular Chemistry and Biochemistry, Faculty of Science and Engineering, Doshisha University, Kyotanabe, Kyoto 610-0321, Japan

ARTICLE INFO

Article history:
Received 24 October 2010
Received in revised form 4 December 2010
Accepted 7 December 2010
Available online 14 December 2010

Keywords:
Molten salt
Thermal battery
Electrolyte
Simulation
Ionic conductivity
Melting point

ABSTRACT

Using a new simulative technique developed by us, we systematically investigated new ternary or quaternary molten salt systems, which are based on LiF–LiCl, LiF–LiBr, and LiCl–LiBr binary systems, for use as electrolytes in thermal batteries, and evaluated their ionic conductivities and melting points experimentally. It was confirmed experimentally that LiF–LiBr–KF (melting point: 425 °C, ionic conductivity at 500 °C: 2.52 S cm^{-1}), LiCl–LiBr–KF (405 °C, 2.56 S cm^{-1}), LiCl–LiBr–NaF–KF (425 °C, 3.11 S cm^{-1}), LiCl–LiBr–NaCl–KCl (420 °C, 2.73 S cm^{-1}), and LiCl–LiBr–NaBr–KBr (420 °C, 2.76 S cm^{-1}) meet our targets for both melting point (350–430 °C) and ionic conductivity (2.0 S cm^{-1} and higher at 500 °C). A single cell using the newly developed LiCl–LiBr–NaCl–KCl molten salt as an electrolyte was prepared, and the DC-IR of the cell decreased by 20% than that of a single cell using the conventional LiCl–KCl molten salt. It was therefore concluded that the use of new quaternary molten salt systems can improve the discharge rate-capability in practical battery applications because of their high ionic conductivities.

1. Introduction

High temperature molten salt batteries, which generally consist of a high temperature molten salt electrolyte (such as LiCl–KCl), a Li–Al alloy anode, and a FeS_2 cathode, have been developed for electric vehicle applications and for use as so-called thermally activated batteries (or thermal batteries), because of their high output power, superior stability in long-term storage, and so on [1–9]. The thermal batteries can produce enormous high power drain due to a high ionic conductivity of the molten salt electrolyte, which is obtained in the liquid state within a proper temperature range of ca. 400–600 °C. Hence the thermal batteries consist of two functional parts. One is the "heat generation system" that generates heat and maintains the molten salt in the liquid state, and the other part is the "electrochemical cell system" that generates electric power [10].

The conventional LiCl–KCl molten salt system, which has been used as an electrolyte in thermal batteries, has a melting point of 350 °C and an ionic conductivity of 1.85 S cm^{-1} at 500 °C. To further improve the discharge rate-capability of the thermal batteries, the molten salt electrolyte should have a higher ionic conductivity and a melting point to be fitted to the conventional heat generation system developed for the LiCl–KCl system [11]. We set the target of the ionic conductivity at 2.0 S cm^{-1} or higher at 500 °C to further increase the output power of the high temperature molten salt batteries, and the target for the melting point within a temperature range of 350–430 °C to replace the conventional LiCl–KCl electrolyte with newly developed electrolyte systems.

In a previous work, we established a simulative technique to predict the ionic conductivity and the melting point to develop new multi-component molten salt systems more effectively [12]. Using this technique, we proposed brand-new quaternary molten salt systems based on the LiF–LiCl–LiBr ternary system, and confirmed that LiF–LiCl–LiBr–0.10KX (X = F, Cl, and Br) systems meet our targets for both the ionic conductivity and the melting point.

In the present study, using this new simulative technique, we systematically investigated new ternary or quaternary molten salt systems based on LiF–LiCl, LiF–LiBr, and LiCl–LiBr binary systems, and experimentally evaluated their ionic conductivities and melting points. Our goal is to find new molten salts systems that contain neither environmentally instable anions such as iodides nor expensive cations such as Rb^+ and Cs^+, and, if possible, that do not contain F^- anions, because the use of F^- anions may be environmentally unfavorable upon disposal as industrial wastes. We finally obtained new quaternary salt systems without F^- anions, i.e. LiCl–LiBr–NaCl–KCl and LiCl–LiBr–NaBr–KBr systems that meet our targets for melting point and ionic conductivity. Furthermore a single cell using the newly developed LiCl–LiBr–NaCl–KCl molten salt as an electrolyte was prepared, and its electrochemical performance was compared with that of a single cell using the conventional LiCl–KCl molten salt.

* Corresponding author. Tel.: +81 6 6991 4639; fax: +81 6 6998 3179.
E-mail address: fujiwara.syozou@jp.panasonic.com (S. Fujiwara).

0378-7753/$ – see front matter © 2011 Published by Elsevier B.V.
doi:10.1016/j.jpowsour.2010.12.009

2. Experimental

2.1. Materials

LiF, LiBr, NaF, NaCl, KF, KCl and KBr from Kanto Kagaku, and LiCl and NaBr from Kojundo Chemical Laboratory were used as raw materials. All these materials were of reagent grade with purity higher than 99.9%. After these salts were dried separately at 200 °C under vacuum for 48 h, they were mixed to obtain various kinds of ternary or quaternary molten salt systems at their eutectic compositions listed in Tables 1–7, which were based on LiF–LiCl, LiF–LiBr, and LiCl–LiBr salt systems.

2.2. Ionic conductivity and melting point measurements

The ionic conductivity of the molten salts was measured by the alternating current (AC) impedance method based on a report by Sato et al. [13]. Prior to measurements, the cell constant K was determined with the LiCl–KCl molten salt that has a well-accepted ionic conductivity (1.85 S cm^{-1} at 500 °C) [14,15]. The ionic conductivity κ was obtained from the measured resistance R of the sample using the following equation:

$$\kappa = K \times R^{-1} \quad (1)$$

The preparation of the molten salts and conductivity measurements were conducted in a glove box filled with dried air. The dew point in the glove box was maintained below −45 °C.

The melting points of the molten salts were determined by differential thermal analysis (DTA) using a TG-DTA system (Bruker Axs, TG-DTA2000SA).

2.3. Simulative technique

Phase diagrams and eutectic compositions of molten salt systems of different compositions and temperatures were calculated from thermodynamic data using a FactSage software (GTT Technologies GmbH), which is based on the CALPHAD (Calculation of Phase Diagram and Thermodynamics) method [16].

The ionic conductivity of a mixed molten salt system was obtained from the equivalent conductivities and the molar ratio of constituent salts at the eutectic composition obtained from the phase diagram of the system using the CALPHAD method [12]. For example, in the case of a ternary salt system consisting of salts 1, 2, and 3, we calculated the apparent equivalent conductivity, the apparent gram equivalent, the apparent density, and the ionic conductivity at a given temperature as follows:

(1) Apparent equivalent conductivity γ_{mix}:

$$\gamma^t_{mix} = X_1 \times \gamma^t_1 + X_2 \times \gamma^t_2 + X_3 \times \gamma^t_3 \quad (2)$$

(2) Apparent gram equivalent eq_{mix}:

$$eq_{mix} = X_1 \times eq_1 + X_2 \times eq_2 + X_3 \times eq_3 \quad (3)$$

Table 1
Comparison of simulated and experimentally obtained data for melting point and ionic conductivity for new LiF–LiCl–NaX (X = F, Cl, and Br) systems developed in the present study.

Molten salt system	Simulated data								Experimental data	
	Eutectic composition (mol%)	Li content (mol%)	Na content (mol%)	F content (mol%)	Cl content (mol%)	Br content (mol%)	Melting point (°C)	Ionic conductivity (S cm^{-1} at 1000 °C)	Melting point (°C)	Ionic conductivity (S cm^{-1} at 500 °C)
LiF–LiCl–NaF	12–77–11	88.9	11.0	23.0	76.9	–	500	7.41	490	3.44
LiF–LiCl–NaCl	23–66–11	88.6	11.4	22.9	77.1	–	495	7.20	495	3.34
LiF–LiCl–NaBr	9–62–29	71.2	28.8	9.1	62.1	29.8	440	5.67	475	3.07

Table 2
Comparison of simulated and experimentally obtained data for melting point and ionic conductivity for new LiF–LiCl–KX (X = F, Cl, and Br) systems developed in the present study.

Molten salt system	Simulated data								Experimental data	
	Eutectic composition (mol%)	Li content (mol%)	K content (mol%)	F content (mol%)	Cl content (mol%)	Br content (mol%)	Melting point (°C)	Ionic conductivity (S cm^{-1} at 1000 °C)	Melting point (°C)	Ionic conductivity (S cm^{-1} at 500 °C)
LiF–LiCl–KF	2–84–14	85.5	14.4	16.5	83.5	–	470	6.83	450	2.65
LiF–LiCl–KCl	2–59–39	60.8	39.1	2.0	97.9	–	360	4.85	350	1.89
LiF–LiCl–KBr	2–60–38	62.4	37.6	2.3	60.1	37.6	375	4.20	350	1.74

Table 3
Comparison of simulated and experimentally obtained data for melting point and ionic conductivity for new LiF–LiBr–NaX (X = F, Cl, and Br) systems developed in the present study.

Molten salt system	Simulated data								Experimental data	
	Eutectic composition (mol%)	Li content (mol%)	Na content (mol%)	F content (mol%)	Cl content (mol%)	Br content (mol%)	Melting point (°C)	Ionic conductivity (S cm^{-1} at 1000 °C)	Melting point (°C)	Ionic conductivity (S cm^{-1} at 500 °C)
LiF–LiBr–NaF	14–79–7	93.5	6.5	20.8	–	79.2	450	6.74	455	3.07
LiF–LiBr–NaCl	13–71–16	84.2	15.8	13.4	15.8	70.8	420	6.40	450	3.11
LiF–LiBr–NaBr	20–73–7	92.5	7.4	20.0	–	80.0	450	6.53	450	3.06

Table 4
Comparison of simulated and experimentally obtained data for melting point and ionic conductivity for new LiF–LiBr–KX (X = F, Cl, and Br) systems developed in the present study.

Molten salt system	Simulated data								Experimental data	
	Eutectic composition (mol%)	Li content (mol%)	K content (mol%)	F content (mol%)	Cl content (mol%)	Br content (mol%)	Melting point (°C)	Ionic conductivity (S cm^{-1} at 1000 °C)	Melting point (°C)	Ionic conductivity (S cm^{-1} at 500 °C)
LiF–LiBr–KF	2–85–13	87.5	12.5	14.7	–	85.3	425	6.49	425	2.52
LiF–LiBr–KCl	3–62–35	64.7	35.3	2.9	35.3	61.8	350	5.18	325	1.73
LiF–LiBr–KBr	3–60–37	62.6	37.4	2.9	–	97.1	330	4.55	320	1.67

Table 5
Comparison of simulated and experimentally obtained data for melting point and ionic conductivity for new LiCl–LiBr–NaX (X = F, Cl, and Br) systems developed in the present study.

Molten salt system	Simulated data								Experimental data	
	Eutectic composition (mol%)	Li content (mol%)	Na content (mol%)	F content (mol%)	Cl content (mol%)	Br content (mol%)	Melting point (°C)	Ionic conductivity (S cm^{-1} at 1000 °C)	Melting point (°C)	Ionic conductivity (S cm^{-1} at 500 °C)
LiCl–LiBr–NaF	25–62–13	86.5	13.5	13.5	24.8	61.7	420	6.65	440	3.22
LiCl–LiBr–NaCl	12–57–31	69.0	31.0	–	43.3	56.7	420	5.97	490	3.33
LiCl–LiBr–NaBr	12–57–31	69.0	31.0	–	43.6	56.4	420	5.56	485	3.42

Table 6
Comparison of simulated and experimentally obtained data for melting point and ionic conductivity for new LiCl–LiBr–KX (X = F, Cl, and Br) systems developed in the present study.

Molten salt system	Simulated data								Experimental data	
	Eutectic composition (mol%)	Li content (mol%)	K content (mol%)	F content (mol%)	Cl content (mol%)	Br content (mol%)	Melting point (°C)	Ionic conductivity (S cm^{-1} at 1000 °C)	Melting point (°C)	Ionic conductivity (S cm^{-1} at 500 °C)
LiCl–LiBr–KF	21–66–13	87.3	12.7	12.7	21.6	65.7	420	6.48	405	2.56
LiCl–LiBr–KCl	30–30–40	59.7	40.3	–	70.1	29.9	365	4.86	360	1.80
LiCl–LiBr–KBr	11–50–39	61.4	38.6	–	11.1	88.9	330	4.44	320	1.71

Table 7
Comparison of simulated and experimentally obtained data for melting point and ionic conductivity for new LiCl–LiBr–NaX–KX quaternary systems (X = F, Cl, and Br) systems developed in the present study.

Molten salt system	Simulated data									Experimental data	
	Eutectic composition (mol%)	Li content (mol%)	Na content (mol%)	K content (mol%)	F content (mol%)	Cl content (mol%)	Br content (mol%)	Melting point (°C)	Ionic conductivity (S cm^{-1} at 1000 °C)	Melting point (°C)	Ionic conductivity (S cm^{-1} at 500 °C)
LiCl–LiBr–NaF–KF	23–63–10–4	84.8	10.0	4.2	14.2	23.3	62.5	415	6.58	425	3.11
LiCl–LiBr–NaCl–KCl	4–59–23–14	63.2	23.5	14.0	0	41.4	58.6	390	5.53	420	2.73
LiCl–LiBr–NaBr–KBr	39–24–24–13	63.9	23.6	12.5	0	39.4	60.6	395	5.02	420	2.76

(3) Apparent density $\rho_{\text{mix}}{}^{t}$:

$$\rho^{t}_{\text{mix}} = X_1 \times \rho^{t}_{1} + X_2 \times \rho^{t}_{2} + X_3 \times \rho^{t}_{3} \quad (4)$$

(4) Ionic conductivity κ_{mix}:

$$\kappa^{t}_{\text{mix}} = \frac{\gamma^{t}_{\text{mix}}}{\text{eq}_{\text{mix}} \times \rho^{t}_{\text{mix}}} \quad (5)$$

Here X_1, X_2, and X_3 denote the mole fractions, $\gamma_1{}^{t}$, $\gamma_2{}^{t}$, and $\gamma_3{}^{t}$ the equivalent conductivities, eq_1, eq_2, and eq_3 the gram equivalents, $\rho_1{}^{t}$, $\rho_2{}^{t}$, and $\rho_3{}^{t}$ the densities of salts 1, 2, and 3, respectively, at a temperature t (K).

The melting point and the molar fraction of each mixed melt were obtained from the eutectic composition of the phase diagram determined with the CALPHAD method, and the equivalent conductivity and the density of each salt were obtained from the literature [14,15]. In the simulation, the ionic conductivity was calculated at 1000 °C because each mono-salt has a high melting point, e.g. LiF (842 °C).

2.4. Preparation of single cell

A single cell shown in Fig. 1, which consisted of a newly developed electrolyte (LiCl–LiBr–NaCl–KCl), a FeS_2 positive electrode, and a Li–Al alloy negative electrode, was prepared to evaluate the performance of the electrolyte. All the procedures for material preparation and cell construction were carried out in dry air with a dew point lower than −45 °C to eliminate the effects of moisture.

The optimized electrolyte salt mixture was crushed using a ball mill with stainless steel balls for about 12 h under Ar atmosphere at a controlled dew point lower than −45 °C, and was classified with a #60 sieve (250-μm mesh). The salt powder was mixed with magnesium oxide (MgO) as a matrix for the electrolyte at a weight ratio

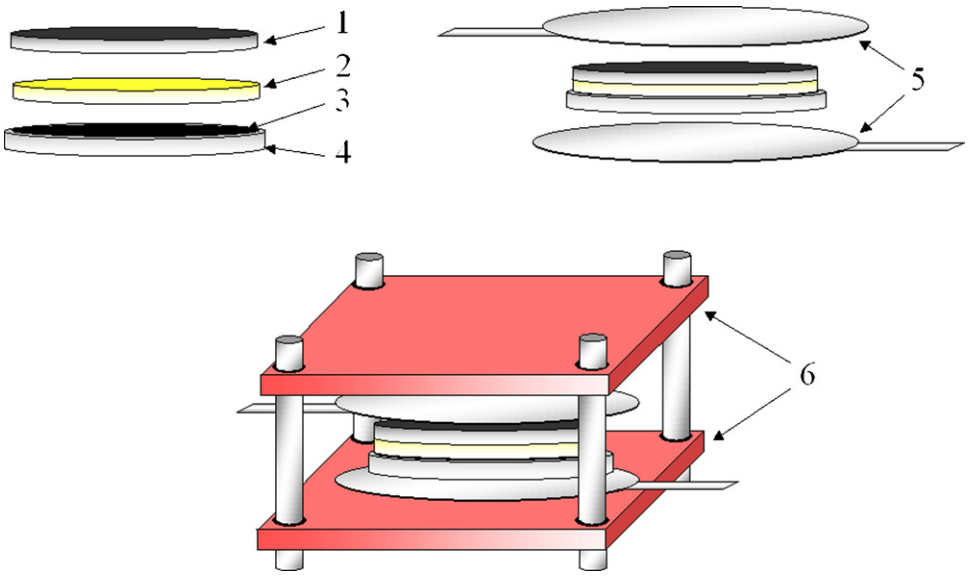

Fig. 1. Schematic illustration of a single cell and test equipment for high-temperature molten-salt batteries. 1: cathode composite, 2: electrolyte composite, 3: anode composite, 4: stainless steel (SUS304) cup, 5: current collector plates (SUS304), 6: hot plates (SUS304).

of 60:40, and the mixture was heated in a melting furnace at 500 °C for 6 h to thoroughly impregnate the salt within the pores of the MgO powder. After cooled, the mixture was again crushed with a ball mill with stainless steel balls for about 12 h under Ar atmosphere, and was classified with a #60 sieve. The obtained mixture powder was pressed with a die at a pressure of 294 MPa to obtain an electrolyte disk of 13-mm diameter and 0.5-mm thickness.

FeS_2 powder (Cerac, reagent grade from, purity >99.9%) was used as a positive electrode active material. The FeS_2 powder, the conventional LiCl–KCl eutectic mixture powder, and silica powder (0.2 μm) were mixed with a weight ratio of 70:20:10. The resulting mixture was pressed with a die at a pressure of 294 MPa to obtain a positive electrode disk of 13-mm diameter and 0.4-mm thickness.

Li–Al alloy powder (Cerac, lithium content: 20 wt%, reagent grade) was used as a negative electrode active material. The Li–Al alloy powder and the conventional LiCl–KCl eutectic mixture powder were mixed with a weight ratio of 65:35. The resulting mixture was pressed with a die at a pressure of 294 MPa to obtain a negative electrode composite of 11-mm diameter and 0.4-mm thickness. The negative electrode layer was placed in a cup made of stainless steel (SUS 304) to obtain a negative electrode disk of 13-mm diameter and 0.5-mm thickness.

The single cell was finally obtained by stacking the positive electrode disk, the electrolyte disk, the negative electrode disk, and current collector plates made of stainless steel as shown in Fig. 1.

2.5. Cell performance test

The single cell was sandwiched between two temperature-controllable stainless steel plates as shown in Fig. 1, and heated to 500 ± 1 °C, and discharge performance was evaluated with an electrochemical test system (BioLogic Science Instruments SP-150). The cell was discharged using consecutive current pulses: 1.0 A cm^{-2} (0.03 s), 2.0 A cm^{-2} (0.03 s), and 4.0 A cm^{-2} (0.03 s) with intervals (0.12 s), which are typical for thermal batteries, and the performance was compared with that of a single cell using the conventional LiCl–KCl electrolyte. The direct current internal resistance (DC-IR) was evaluated during the discharge using the following equation:

$$\text{DC-IR} = \frac{V_{\text{open}} - V_x}{I_x} \quad (6)$$

Here V_{open} denotes the open-circuit voltage (at no load), I_x the current at a current density of x A cm^{-2} (x = 1, 2, or 4) and V_x the cell voltage at x A cm^{-2}.

3. Results and discussion

3.1. New ternary molten salt systems

In the present study, we chose LiF–LiCl, LiF–LiBr, and LiCl–LiBr binary systems as base salt systems, and NaF, NaCl, NaBr, KF, KCl, and KBr from alkaline halides as the third salt to prepare new types of ternary molten salt systems, most of which have not been reported yet. Here we excluded alkaline halides containing environmentally instable anions such as iodides and expensive cations as Cs^+ and Rb^+ as the third salt. The effects of the third salt addition on the ionic conductivity and the melting point of the resulting ternary molten salt systems were discussed.

3.1.1. LiF–LiCl–NaX and LiF–LiCl–KX (X = F, Cl, and Br) systems

Simulated data for the eutectic compositions, the ionic conductivities (at 1000 °C), and the melting points of the LiF–LiCl–NaX and LiF–LiCl–KX (X = F, Cl, and Br) systems are listed in Tables 1 and 2, respectively, as well as the ionic conductivities (at 500 °C) and the melting points obtained experimentally. The simulated data for LiF–LiCl–NaX (X = F, Cl, and Br) systems suggested that these new ternary molten salt systems have higher melting points (≥440 °C) than our target (350–430 °C), which were confirmed experimentally. Because the elemental compositions of the LiF–LiCl–NaF and LiF–LiCl–NaCl systems are nearly equal to each other, they have the same eutectic composition. The two systems have very high melting points of ca. 500 °C. These high melting points were brought about by the anion effect of the F^- described in a previous report [12]; i.e. the addition of a large amount of the F^- anion, especially >20 mol%, increases the melting point. This is because F^- anions have the smallest ionic radius among the anions used in the present study, and hence the effect of F^- anions on the total stability of the crystal structure in the solid state is the weakest [12].

The simulated melting point of the LiF–LiCl–NaBr system was relatively low (440 °C), but the experimentally measured one (475 °C) was significantly higher than that the simulated one. Similar anomaly in the presence of a large amount of Na^+ cations was

observed for the quaternary LiF–LiCl–LiBr–0.30NaCl system in our previous study [12]. Though the reason is not clear at present, there may be an effect of inhomogeneity during the crystallization process, owing to kinetically fast crystallization of an unknown phase containing Na^+ cations [12].

For the LiF–LiCl–KX (X = F, Cl, and Br) systems, the melting points and the tendency of the ionic conductivity obtained experimentally well agreed with the simulated data. The LiF–LiCl–KF system showed a higher melting point than the LiF–LiCl–KCl and the LiF–LiCl–KBr systems. The low melting points of the LiF–LiCl–KCl and the LiF–LiCl–KBr systems are attributable to the high content (37.6 and 39.1 mol%, respectively) of K^+ cations at their eutectic compositions. The large K^+ cations (1.38 Å) reduce the total stability of the crystal structure in the solid states more significantly than Li^+ or Na^+ cations (0.76 and 1.02 Å, respectively), and this effect resulted in lowering the melting point [12]. However, the addition of larger K^+ cations lowers the ionic conductivity as shown in Table 2, which is also due to the large size of K^+ cations.

Neither LiF–LiCl–NaX nor LiF–LiCl–KX (X = F, Cl, and Br) system satisfied our targets for melting point (350–430 °C) and ionic conductivity ($\geq$2 S cm^{-1} at 500 °C).

3.1.2. LiF–LiBr–NaX and LiF–LiBr–KX (X = F, Cl, and Br) systems

Simulated data for the eutectic compositions, the ionic conductivities (at 1000 °C), and the melting points of the LiF–LiBr–NaX and LiF–LiBr–KX (X = F, Cl, and Br) systems are listed in Tables 3 and 4, respectively, as well as the ionic conductivities (at 500 °C) and the melting points obtained experimentally. The simulated data for the LiF–LiCl–NaX (X = F, Cl, and Br) systems suggested that the LiF–LiCl–NaF and LiF–LiCl–NaBr systems, which seem to have the same eutectic compositions, have a high melting point of 450 °C. The high melting point is due to the high content of F^- anions (20.0–20.8 mol%) at the eutectic compositions as described in the previous section. In the case of the LiF–LiCl–NaCl system, the simulated melting point was low (420 °C), but the experimentally measured melting point (450 °C) is significantly higher than the simulated one. This is due to the high content of Na^+ cations (15.8 mol%) as discussed in the previous section.

For the LiF–LiBr–KX (X = F, Cl, and Br) systems, the melting points and the tendency of the ionic conductivity obtained experimentally well agreed to the simulated data. The LiF–LiBr–KCl and the LiF–LiBr–KBr systems had very low melting points, which were brought about by the K^+ cation effect as discussed in the previous section. However, the high content of K^+ cations (35.3 and 37.4 mol%, respectively) lowered the ionic conductivity. The LiF–LiBr–KF system had a low melting point (425 °C) and a high ionic conductivity (2.52 S cm^{-1}), which satisfied our targets for melting point (350–430 °C) and ionic conductivity ($\geq$2 S cm^{-1} at 500 °C). This is probably because the system has a suitable content of K^+ cations (12.5 mol%) at the eutectic composition.

3.1.3. LiCl–LiBr–NaX and LiCl–LiBr–KX (X = F, Cl, and Br) systems

Simulated data for the eutectic compositions, the ionic conductivities (at 1000 °C), and the melting points of the LiCl–LiBr–NaX and LiCl–LiBr–KX (X = F, Cl, and Br) systems are listed in Tables 5 and 6, respectively, as well as the ionic conductivities (at 500 °C) and the melting points obtained experimentally. Simulated data for the LiCl–LiBr–NaX (X = F, Cl, and Br) systems suggested that they have a low melting point (420 °C). However, the experimentally measured melting points (440–490 °C) were much higher than the simulated ones, which is again due to the high content of Na^+ cations (13.5–31.0 mol%) as discussed in the previous sections. The LiCl–LiBr–NaCl and the LiCl–LiBr–NaBr systems have the same eutectic compositions, because the elemental compositions are nearly equal to each other.

For the LiCl–LiBr–KX (X = F, Cl, and Br) systems, the melting points and the tendency of the ionic conductivity obtained experimentally well agreed to the simulated data. The LiCl–LiBr–KCl and LiCl–LiBr–KBr systems showed very low melting points, which were brought about by the high content of K^+ cations (40.3 and 38.6 mol%, respectively). Only the LiCl–LiBr–KF system (m.p.: 405 °C, κ: 2.56 S cm^{-1}) satisfied our targets for melting point (350–430 °C) and ionic conductivity ($\geq$2 S cm^{-1} at 500 °C). This is again due to a suitable content of K^+ cation (12.7 mol%) at the eutectic composition as was found for the LiF–LiBr–KF system in the previous section.

3.2. New quaternary molten salt systems: LiCl–LiBr–NaX–KX systems (X = Cl, and Br)

Of the six ternary system investigated in the previous sections, only two systems, LiF–LiBr–KF (m.p.: 425 °C, κ: 2.52 S cm^{-1}), LiCl–LiBr–KF (m.p.: 405 °C, κ: 2.56 S cm^{-1}) meet our targets for melting point (350–430 °C) and ionic conductivity ($\geq$2 S cm^{-1} at 500 °C). We also found several specific effects of anions and cations in the multi-salt systems; for example, the addition of F^- anions and Na^+ cations increases the melting point, while the addition of K^+ cations decreases the melting point of the multi-salt system, but significantly decreases the ionic conductivity. A high content of F^- anions and Na^+ cations resulted in a high melting point and a high content of K^+ cations resulted in a low ionic conductivity. The above two systems that meet our targets probably contain K^+ cations and F^- anions at preferable (i.e. not too high) contents (12–15 and 12–13 mol%, respectively).

As mentioned above, Na^+ and K^+ cations have the opposite effects for the melting point; the former increase and the latter decrease the melting point. Hence we investigated further possibility of new quaternary molten salt systems based on the LiCl–LiBr–NaX–KX (X = F, Cl, and Br) ternary salt systems, which have not been reported yet to the best of our knowledge. Our final goal was to find the possibility of a new molten salt system without F^- anions that satisfy our target of the melting point and the ionic conductivity, because the use of F^- anions may be environmentally unfavorable upon disposal as industrial wastes.

Simulated data for the eutectic compositions, the ionic conductivities (at 1000 °C), and the melting points of the LiCl–LiBr–NaX–KX (X = F, Cl, and Br) quaternary salt systems are listed in Table 7, as well as the melting points and the ionic conductivities (at 500 °C) obtained experimentally. All the quaternary salt systems satisfied our targets for melting point (350–430 °C) and ionic conductivity ($\geq$2 S cm^{-1} at 500 °C). In particular, the LiCl–LiBr–NaCl–KCl and LiCl–LiBr–NaBr–KBr systems are attractive as electrolytes for the thermal batteries, because they do not contain environmentally unfavorable F^- anions.

3.3. Cell performance of a single cell using a newly developed molten salt system

We prepared a single cell using the LiCl–LiBr–NaCl–KCl system as an electrolyte, and investigated the cell performance. The cell was heated to 500 °C, and its performance was measured using consecutive current pulses of 1.0, 2.0 and 4.0 A cm^{-2}, which are typical current densities for thermal batteries. The pulse discharge performance of the single cells using the conventional LiCl–KCl electrolyte (1.85 S cm^{-1} at 500 °C) and the newly developed LiCl–LiBr–NaCl–KCl electrolyte (2.73 S cm^{-1} at 500 °C) are compared in Fig. 2, and the DC-IR values at different current densities are summarized in Table 8. We confirmed that discharge characteristics of a single cell using a new quaternary molten salt system, LiCl–LiBr–NaCl–KCl as its electrolyte are improved significantly, and the DC-IR was by 20–27% lower than that of the cell

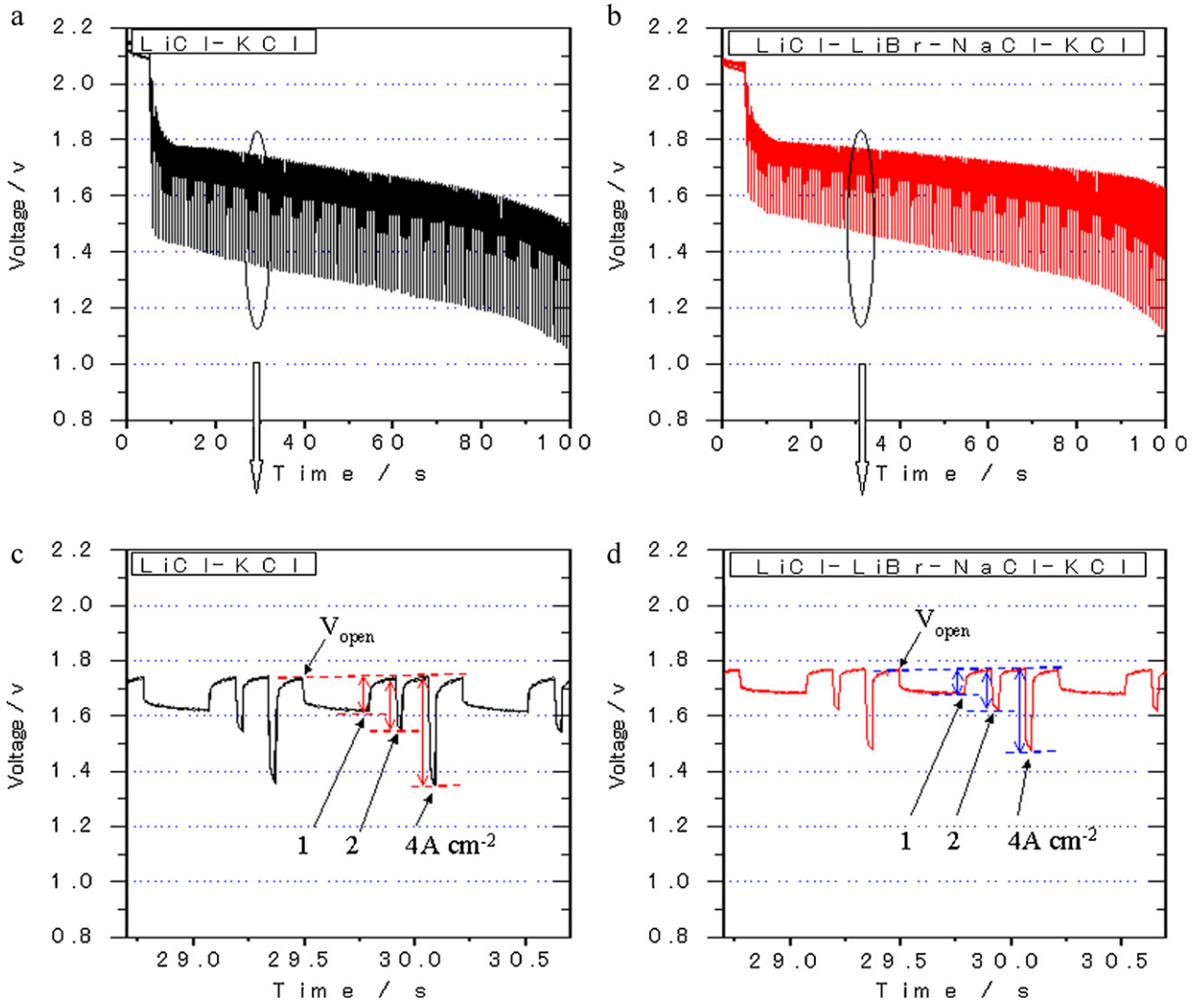

Fig. 2. Pulse discharge curves (a and b) and their magnified curves (c and d) of single cells using (a and c) the conventional LiCl–KCl system and (b and d) the newly developed LiCl–LiBr–NaCl–KCl system as electrolytes. Positive electrode: FeS_2; negative electrode: Li–Al alloy, temperature: 500 ± 1 °C.

Table 8
Comparison of discharge performance of single cells using the conventional LiCl–KCl system and the newly developed LiCl–LiBr–NaCl–KCl system as electrolytes (500 °C).

Current density (A cm^{-2})	LiCl–KCl DC-IR (mΩ)			LiCl–LiBr–NaCl–KCl DC-IR (mΩ)		
	15 s	30 s	60 s	15 s	30 s	60 s
1	75.8	85.7	92.6	57.2 (−24.6%)	63.4 (−26.1%)	67.8 (−26.8%)
2	65.1	67.9	73.8	48.4 (−25.8%)	54.0 (−20.4%)	59.2 (−19.8%)
4	64.7	71.7	74.4	47.3 (−26.8%)	55.0 (−23.3%)	59.9 (−19.6%)

Values within the parenthesis indicate the improvement in DC-IR for the LiCl–LiBr–NaCl–KCl electrolyte system compared with that for the conventional LiCl–KCl.

using the conventional LiCl–KCl molten salt system over a wide electric current density range (1.0, 2.0, and 4.0 A cm^{-2}) during a discharging time of 60 s, which is required for typical use of the thermal batteries. It is therefore concluded that the use of newly developed quaternary molten salt systems can improve the discharge rate-capability in practical battery applications because of their high ionic conductivities.

4. Conclusions

To improve discharge rate-capability of high temperature molten salt batteries, novel ternary or quaternary molten salt systems based on LiF–LiCl, LiF–LiBr, and LiCl–LiBr binary systems, were investigated without adding environmentally instable anions such as iodides or expensive cations such as Cs^+ and Rb^+. To estimate the ionic conductivities and the melting points of multi-component molten salts systems and to develop new molten salt systems more effectively, we used a simulative technique using the CALPHAD method developed in our previous work.

It was confirmed experimentally that LiF–LiBr–KF (m.p.: 425 °C, κ at 500 °C: 2.52 S cm^{-1}), LiCl–LiBr–KF (405 °C, 2.56 S cm^{-1}), LiCl–LiBr–NaF–KF (425 °C, 3.11 S cm^{-1}), LiCl–LiBr–NaCl–KCl (420 °C, 2.73 S cm^{-1}), and LiCl–LiBr–NaBr–KBr (420 °C, 2.76 S cm^{-1}) meet our targets for melting point (350–430 °C) and ionic conductivity (≥2.0 S cm^{-1} at 500 °C). In particular, the quaternary systems, LiCl–LiBr–NaCl–KCl and LiCl–LiBr–NaBr–KBr, are attrac-

tive as electrolytes for the thermal batteries, because they do not contain environmentally unfavorable F^- anions.

We confirmed that the DC-IR of the single cell using the new quaternary molten salt system, LiCl–LiBr–NaCl–KCl, as its electrolyte was by more than 20–27% lower than that using the conventional LiCl–KCl molten salt system within a wide electric current density range (1.0, 2.0, and 4.0 A cm^{-2}) during a discharging time of 60 s, which is required for typical use of the thermal batteries.

It is therefore concluded that the new simulative technique with the CALPAHD method is a powerful tool to estimate the important characteristics of molten salt electrolytes such as the ionic conductivity and the melting point, and that the new molten salt systems developed using the simulative technique are very promising for the improvement of the discharge rate-capability of practical battery applications because of their high ionic conductivities.

References

[1] T.D. Kaun, M.C. Hash, G.L. Henriksen, A.N. Jansen, D.R. Vissers, Materials and mechanisms of high temperature lithium sulfide batteries, in: Conference: 2. Chilean Lithium Symposium, Santiago (Chile), 1994, pp. 171–192.
[2] T.D. Kaun, P.A. Nelson, L. Redey, D.R. Vissers M, G.L. Henriksen, High temperature lithium/sulfide batteries, Electrochim. Acta 38 (9) (1993) 1269–1287.
[3] R.A. Guidotti, Thermal batteries: a technology review and future directions, in: The 27th International Technical Conference of the Society for the Advancement of Material and Process Engineering (SAMPE): Diversity into the Next Century, Albuquerque, NM, 1995, pp. 807–818.
[4] A.G. Ritchie, P. Carter, Thermal stability of iron disulphide, FeS_2, cathode material in thermal batteries, in: The 38th Power Sources Conference, Cherry Hill, New Jersey, 1998, pp. 215–218.
[5] R.A. Guidotti, G.L. Scharrer, F.W. Reinhardt, Development of a high-power and high-energy thermal battery, in: The 39th Power Sources Conference, Fort Monmouth, New Jersey, 2000, pp. 547–551.
[6] P. Masset, Iodide-based electrolytes: a promising alternative for thermal batteries, J. Power Sources 160 (1) (2006) 688–697.
[7] P. Masset, A. Henry, J.Y. Poinso, J.C. Poignet, Ionic conductivity measurements of molten iodide-based electrolytes, J. Power Sources 160 (1) (2006) 752–757.
[8] P. Masset, J.-Y. Poinso, J.-C. Poignet, Iodide-base electrolytes: an alternative for high-temperature batteries, in: The 41st Power Sources Conference, Philadelphia, Pennsylvania, 2004, pp. 137–140.
[9] P. Masset, S. Schoeffert, J.Y. Poinso, J.C. Poignet, LiF–LiCl–LiI vs. LiF–LiBr–KBr as molten salt electrolyte in thermal batteries, J. Electrochem. Soc. 152 (2) (2005) A405–A410.
[10] S. Fujiwara, New molten salt systems for thermal batteries, in: The 43rd Power Sources Conference, Philadelphia, Pennsylvania, 2008, pp. 121–124.
[11] S. Fujiwara, F. Kato, S. Watanabe, M. Inaba, A. Tasaka, New iodide-based molten salt systems for high temperature batteries, J. Power Sources 194 (2) (2009) 1180–1183.
[12] S. Fujiwara, M. Inaba, A. Tasaka, New molten salt systems for high-temperature molten salt batteries: LiF–LiCl–LiBr-based quaternary systems, J. Power Sources 195 (22) (2010) 7691–7700.
[13] Y. Sato, A. Kojima, T. Ejima, Electric conductivity and density of molten NaF–AlF_3 system, J. Jpn. Inst. Met. 41 (12) (1977) 1249–1256 (in Japanese).
[14] G.J. Janz, F.W. Dampier, G.R. Lakshminarayanan, P.K. Lorenz, R.P.T. Tomkins, Molten Salts: Volume 1, Electrical Conductance, Density, and Viscosity Data, National Standard Reference Data Series (NSRDS), National Bureau of Standards (NBS) 15, 1968, pp. 114–119.
[15] G.J. Janz, R.P.T. Tomkins, C.B. Allen, J.R. Downey Jr., G.L. Gardner, U. Krebs, S.K. Singer, Molten salts: volume 4, part 2, chlorides and mixtures, electrical conductance, density, viscosity, and surface tension data, JPCRD (1975) 871–1178.
[16] L. Kaufman, H. Bernstein, Computer Calculation of Phase Diagrams with Special Reference to Refractory Metals, Academic Press, New York, 1970, pp. 1–334.